

# Diffusing-wave spectroscopy

Georg Maret

Since its invention about a decade ago, dynamic multiple light scattering has found many applications in various areas of soft condensed matter science. It has become a particularly important quantitative tool in colloid physics because of its applicability to systems containing very high concentrations of scatterers, and its extreme sensitivity to small motions. Recent advances of this technique, currently called diffusing-wave spectroscopy because of the diffusive transport of the light waves, include remote optical measurements of frequency-dependent viscoelasticity, studies of the microscopic dynamical processes in flowing sand and aging foam, a theoretical description of dynamic scattering from orientational fluctuations in liquid crystals and imaging of dynamic heterogeneities buried inside a turbid background medium.

## Addresses

Fakultät für Physik, Universität Konstanz POB 5560, D-78434 Konstanz, Germany; e-mail: georg.maret@uni-konstanz.de

Current Opinion in Colloid & Interface Science 1997, 2:251–257

## Abbreviation

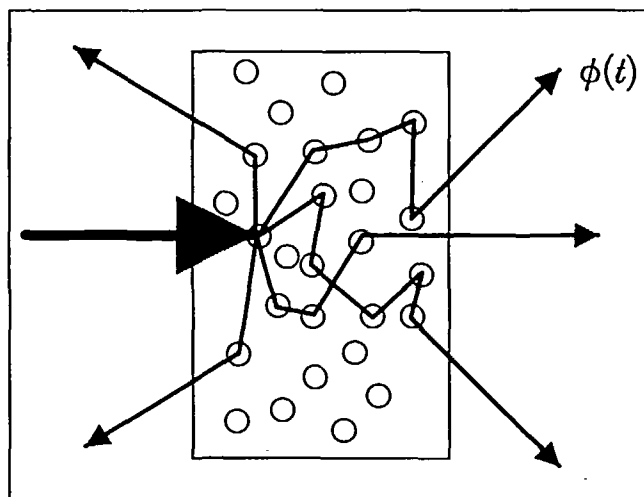
DWS diffusing-wave spectroscopy

## Introduction

Most objects in nature strongly scatter visible light. White paints, milk, many dairy products, snow or clouds are examples where scattering largely dominates over absorption, whereas many biological tissues, wood, rocks, mud, and so on, have substantial absorption in addition to scattering. The turbid opaque appearance of the former list of materials originates from strong scattering of light that, in turn, is caused, usually, by a high concentration of inhomogeneities such as particles suspended in a background medium of rather different refractive index. The scattering is strongest for large index mismatch and for particles of sizes of order of the wavelength of light. Then, as sketched in Figure 1, the impinging light is scattered several or many times before it can escape from the material. In many cases, the transport of light is well described by diffusive spreading of the intensity, or photon diffusion, or photon random walks. The latter is characterized by a photon transport mean free path  $l^*$  (or average random walk step length) which is usually much smaller than the size  $L$  of the object.  $L \gg l^*$  is the criterion for multiple scattering.

Although the photon diffusion picture was introduced almost 100 years ago [1], a rapid development of the field of optical multiple scattering has set in with the discovery

Figure 1



Dynamic multiple scattering of light. The light waves diffusing through the multiple scattering medium pick up phase shifts ( $\phi(t)$ ) due to the motion of the scatterers.

of interference effects such as weak localization [2] and coherent backscattering [3,4] of light. This article focuses on recent work concerning the temporal fluctuations of the multiply scattered light intensity which are caused by motion of the scatterers. Although parts of the underlying physics were discussed previously in 1983 and 1984 [5,6], dynamic multiple light scattering has been reintroduced and highlighted by the work on calibrated colloidal latex particles in aqueous suspensions [7,8] and has been rapidly evolving ever since into a powerful technique called 'diffusing-wave spectroscopy' (DWS).

The principle and mathematical treatment of DWS can be found in various reviews (see e.g. [9,10]). We therefore only briefly resume the physics (Fig. 1): coherent light waves (of, say, an incident monomode laser beam) travel inside the sample along the various random scattering paths described by the photon random walk, and set up a highly irregular intensity pattern called 'speckle', as a result of interference between many waves from many paths of various lengths, at the detector. Similar to conventional dynamic single scattering, the intensity in a given speckle spot fluctuates when the scatterers move with respect to each other. As the transit time of photons through a typical multiple scattering path is much shorter than the time,  $\tau_0$ , it takes a colloidal particle to move a distance of order of the optical wavelength  $\lambda_0 = 2\pi/k_0$  ( $\tau_0 = 1/Dk_0^2$  for Brownian motion with diffusion coefficient  $D$ ), the problem is treated in a quasi-stationary approximation. The time-dependent phase shifts  $\phi(t)$  of the scattered optical fields, occurring due to motion

of scatterers, accumulate along the paths and give rise to speckle fluctuations on a path-length dependent time scale. Consequently, under circumstances of strong multiple scattering, this time scale is much faster than  $\tau_0$ . Unlike single scattering, the time scale does not depend on the angle of observation, but rather on the geometry of the scattering cell which controls the typical path length and its distribution. The seemingly complicated calculation of measurable quantities, like the frequency spectrum or the time autocorrelation function of the scattered intensity, becomes in fact rather straightforward in the photon diffusion picture. For independent random paths, all interference contributions between different paths average to zero and the average relaxation time of paths of  $n$  independent scattering events becomes  $n\tau_0$ . This is seen in the important, fundamental equation for the autocorrelation function of the scattered field [7]:

$$g_1(t) = \int_{l^*}^{\infty} P(s) e^{-\frac{t}{\tau^*} \langle \delta\phi^2(t) \rangle} ds / \int_{l^*}^{\infty} P(s) ds \quad (1)$$

where  $\langle \delta\phi^2(t) \rangle$  is the mean square phase shift per scattering event and  $P(s)$  is a quantity depending on sample geometry, size and  $l^*$ , describing how much light intensity is scattered on average into paths of length  $s$ .  $\langle \delta\phi^2(t) \rangle = k_0^2 \langle \delta r^2(t) \rangle = Dk_0^2 t$  for independent Brownian motion of scatterers with mean square displacement  $\langle \delta r^2(t) \rangle$ . Explicit formulas for  $P(s)$  and hence  $g_1(t)$  have been worked out for various geometries, such as backscattering and transmission from slabs, pairs of optical fibers dipping into a turbid sample and others, and Equation 1 was successfully tested experimentally on suspensions of well characterized colloidal suspensions. See, for example, [9,10].

DWS has tremendously extended the use of light scattering in many fields, in particular in the physics and chemistry of colloids and other complex fluids. Primarily, it provides, without the need for index matching, quantitative information about particle displacements  $\langle \delta r^2(t) \rangle$  up to high concentrations—well in the regime of high order multiple scattering. It works best when single and low order scattering are negligible, and therefore ideally complements other recently developed techniques such as two-color cross-correlation spectroscopy [11] and single-mode fiber-optic dynamic light scattering [12–14], both of which essentially suppress the multiple scattered light but still require measurable amounts of single scattering intensity. DWS is therefore well suited to study interparticle correlations in colloidal suspensions at very high volume fractions and the dynamics of dense-packed systems like concentrated emulsions, foams and so on. The second important feature of DWS is its extraordinary sensitivity to small displacements of scatterers. In contrast to single light scattering, which probes fluctuations on length scales larger than  $\lambda/2$ ,

displacements as small as  $\lambda/1000$  (or even less, in principle) can be monitored with DWS. The probed length scale is easily controlled experimentally by the typical path length (i.e. the maximum of  $P(s)$ ) which is set by the sample size, shape and distance between injection and detection point of the light. Examples below highlight fluctuations measurable at length scales down to about 0.1 nm. This puts DWS in competition with X-ray and neutron scattering, but covering time scales from tens of nanoseconds to hundreds of seconds. The third important feature of DWS is that DWS experiments on other types of motion, such as shear or oscillatory flow, demonstrate the possibility to characterize flow fields and measure velocity gradients on the experimentally adjustable length scale  $l^*$ . Fourthly, because of the high sensitivity to motion of scatterers, DWS can detect very small numbers of particles undergoing motion with respect to their surroundings, thus making it possible to image or localize them even well below the surface of the sample, and to detect sporadic and rare dynamic events. Last, but not least, DWS is easier than dynamic single light scattering to implement experimentally, because of the intrinsically high scattered intensities and the rather weak sensitivity to misalignment and definition of scattering angle, beam size and polarization.

Despite discussions about the accuracy of current DWS theories [15] and difficulties with the proper description of incident and diffusing light near the sample surface [16–19], it seems fair to say that DWS is by now well established to provide quantitative information, to within a few % accuracy, about  $\langle \delta r^2(t) \rangle$ ,  $D$ , particle sizes, flow rates, ultrasonic amplitudes, and so on, for homogeneous multiple scattering media, if the few relevant experimental parameters (sample geometry,  $L$ ,  $l^*$ , ...) are well controlled. Recent illustrations for this are given in the section entitled *DWS on homogeneous colloidal systems*, whereas the two sections following on from this deal with novel developments into more complex inhomogeneous systems and multiple scattering imaging of objects in motion.

## DWS on homogeneous colloidal systems

### Short-time hydrodynamics

DWS experiments [20–22] on the short-time crossover from ballistic to Brownian motion of colloidal spheres have clearly revealed a long-time tail in the velocity auto-correlation function and a scaling of its characteristic time scale with the high frequency shear viscosity of the solution up to high volume fractions due to hydrodynamic interactions. These experiments were carried out on relatively large spheres (of diameters from 0.2 to above 1  $\mu\text{m}$ ), in which case DWS gives access to short time ‘self’ motion of the particles. For particles significantly smaller than  $\lambda$ , DWS rather provides information on the time-dependent ‘collective’ motion, which shows similar features [23,24] including the scaling behavior with the solution viscosity. A striking result of this work

was that the motion of a given particle senses the macroscopic viscosity even at times too short for the vorticity generated by it to diffuse across the average interparticle distance. Analysis of the temporal evolution of the flow field surrounding the particle [25<sup>\*</sup>], and comparison of the latter experiments with numerical simulations [24] suggest that sound propagation plays a major role in the establishment of the hydrodynamic interactions at short times. The discussed scaling behavior remains, however, poorly understood so far.

### Interparticle correlations and phase transitions

The effects of short range interparticle interactions can be easily incorporated into the simple DWS theory (Eq. 1) [7,26] in the case of weak multiple scattering,  $k_0 l^* \gg 1$ . The multiple scattering is then described by successive scattering events from correlated ensembles of scatterers. The correlations modify both the transport mean free path  $l^*$  and the time scale of the intensity fluctuations. The latter reflects the effect of hydrodynamic interaction on the diffusion constant and the fact that in multiple scattering all quantities become averages over a wide distribution of (single) scattering angles. The influence of interactions becomes most pronounced at high volume fractions and small particle sizes, but essentially disappears for particles above  $\approx 1 \mu\text{m}$  diameter. This has been checked by DWS experiments for hard, monodisperse spheres [27–29] up to volume fractions near 50%, binary mixtures of them [30] and charged spheres [31]. At stronger interactions, as achieved either by even higher particle concentrations or by more long range interparticle potential (e.g. screened Coulomb interaction), colloidal suspensions undergo transitions into crystalline or glassy phases depending on the degree of monodispersity of the spheres. These transitions are clearly visible by the appearance of a nondecaying part in  $g_1(t)$  at long times. Although DWS is, in this sense, very useful to establish phase diagrams [32–34], a proper description of the long time behavior of  $g_1(t)$  in DWS from strongly interacting systems is still missing.

### Convective motions

DWS is sensitive to relative motions of scatterers other than Brownian motion, as first illustrated by  $g_1(t)$  measurements on latex suspensions under Poiseuille flow [35]. If the displacements of the particle  $\delta \vec{r}_i$  are completely correlated due to a deterministic motion such as convective flow, the relevant phase shift  $\delta\phi$  due to two successive scattering events ( $i$ ) and ( $i+1$ ) in the expression (Eq. 1) for  $g_1(t)$  is  $\vec{k}_i(\delta \vec{r}_i - \delta \vec{r}_{i+1})$ . As  $\delta \vec{r}_i = \vec{v}_i t$ , it immediately follows that a homogeneous velocity field  $\vec{v}_i$  ( $=\text{constant}$ ), does not generate temporal speckle fluctuations. Inhomogeneous velocities, however, cause phase fluctuations, thereby generating a decay of  $g_1(t)$ . The phase fluctuations are given by the velocity difference on the length  $l^*$ , because consecutive random scattering events have, on average, a distance  $l^*$ . For homogeneous shear at rate  $\Gamma$  one again finds the familiar

expression (Eq. 1) for  $g_1(t)$ , the mean square phase shift per scattering event now being  $\langle \delta\phi^2 \rangle = (\Gamma l^* k_0 t)^2$ . The  $t^2$ -dependence of  $\langle \delta\phi^2 \rangle$  as opposed to the  $t$ -dependence for Brownian motion, is the signature of the deterministic nature of the shear motion. For inhomogeneous shear gradients, such as Poiseuille flow or plug flow, the decay of  $g_1(t)$  becomes somewhat different as the cloud of diffusing photons does not scan the different regions of the flow field with equal weight [36]. Experiments comparing planar flow, Poiseuille flow and Couette flow [37] clearly demonstrate this, and are in quantitative agreement with theory. It is thus possible to distinguish between different types of flow and to determine shear gradients in totally turbid liquids by dynamic multiple light scattering. The Couette flow experiments have been extended to higher shear gradients well into the regime of hydrodynamic instabilities [37]. Beyond a critical shear rate, a characteristic convective roll pattern ('Taylor' rolls) appears. The associated additional shear is clearly seen in  $g_1(t)$ , and scanning the position of a tightly focused incident beam allows one to visualize the otherwise not visible rolls through the position-dependence of the characteristic relaxation rate  $\Gamma l^* k_0$ . These experiments are readily extended to turbulent flow, thus opening the possibility of scale-dependent measurements of  $\langle \Gamma^2 \rangle$  [38].

Small longitudinal relative displacements of the particles can also be detected with the help of DWS. This is illustrated by DWS measurements of the variance of the ac-electrophoretic mobility in electro-rheological fluids [39] and of the ultrasound-generated sinusoidal modulation of the particle positions, from which the ultrasound amplitude could be estimated optically in solid or liquid multiple scattering media [40].

### Towards more complex systems

After the experimental establishment of DWS on well characterized model suspensions, more complex turbid systems have begun to be studied. We emphasize here emulsions, foams, flowing sand, fluidized beds and nematic liquid crystals.

### Shape fluctuations in emulsion droplets and DWS measurements of viscoelasticity

Very dense suspensions of monodisperse emulsion droplets were investigated by Gang *et al.* [41,42]. Thermally excited droplet shape fluctuations with amplitudes as small as a few Å at droplet sizes above  $1 \mu\text{m}$  could be detected. With increasing volume fraction, the characteristic frequency of the fluctuations decreases but, perhaps more surprisingly, their amplitude increases reflecting possibly the increasing importance of thermal collisions between deformable droplets. More recently, these measurements of  $\langle \epsilon^2(t) \rangle$  were extended to entangled polymer solutions containing colloidal probe particles, and to colloidal suspensions of hard spheres at high volume fraction [43<sup>\*\*</sup>,44].  $\langle \epsilon^2(t) \rangle$  is then related to the corresponding bulk storage ( $G'$ ) and loss ( $G''$ ) moduli through a generalized Langevin

equation; the optically obtained values of  $G'$  and  $G''$  agree surprisingly well with direct measurements for all systems studied over the entire frequency range covered. Although the physical reason for this agreement remains to be understood, these measurements, which have been extended to higher frequencies covering up to seven decades [45], can be considered to be a new important application of DWS in complex fluids.

#### Dynamic processes in foams and gelation

Foams belong to a class of materials with structural features and optical properties that are very different to those of dense colloidal suspensions, despite their overall 'white' appearance in many cases. Dense collections of (air) bubbles are separated by more or less organized soap films and hence the multiple scattering of light cannot be described by scattering from large spheres, but rather should be modeled by multiple reflections from more or less random surfaces. Coarsening and aging of foams has been studied experimentally since 1991 [46,47]; the overall slow dynamics has been described as a stochastic sequence of bubble rearrangement events which are easily detected by the large extension of the diffuse photon cloud, despite the rare occurrence of rearrangements. This concept was used more recently to study the rate and stress dependence of bubble rearrangement events in foams flowing under shear [48–50]. The additional dynamics occurring at times much shorter than the rearrangement times is presumably due to thermal shape fluctuations of the bubbles [51], and can be understood in terms of the macroscopic shear modulus.

Other examples of how DWS, while probing fast fluctuations (on the microsecond to millisecond time scale), can be used to study very slow processes (on hour scales) is the monitoring of gelation of milk by rennet action at an early stage in cheese production [52], or the temporal evolution of colloidal gels [53].

#### Fluidized beds and flowing sand

Fluidized beds are suspensions of large spheres which are kept from sedimenting by upwards directed flow. DWS has been used to study the effect of hydrodynamic interactions on the average sedimentation velocity—its variance and diffusion in uniform hard sphere fluidized suspensions [54]. Very recently, a study [55\*\*] of flowing sand has revealed a surprisingly rich dynamic behavior of such systems: at short times, the motion of sand grains is ballistic and has velocity fluctuations comparable to the average velocities, and the measured grain collision time and mean free path reveal a very small dilatation; at later times, a subdiffusive motion which is related to the distortion of nearest neighbor cages of sand grains is observed.

#### Liquid crystals

Single light scattering from macroscopically oriented nematic liquid crystals is well understood and can be found in

many textbooks. It arises from collective orientation fluctuations of molecules with anisotropic optical polarizability ( $\delta\epsilon/\epsilon$  does not equal 0). The statics and dynamics of these fluctuations are described in a continuum-elastic model involving several elastic constants ( $\kappa$ ) and viscosities ( $\eta$ ). In the one-constant approximation, the amplitude of the light scattered at wave vector  $q$  is proportional to  $(\delta\epsilon/\epsilon)^2 k_0^4 kT/(\kappa q^2)$  where  $kT$  has the usual meaning. The corresponding relaxation time is  $(\kappa q^2/\eta)^{-1}$ , very similar to Brownian motion  $(Dq^2)^{-1}$ , with  $\kappa/\eta \equiv D$ . Both scattering amplitude and relaxation time diverge for long wavelengths ( $q \rightarrow 0$ ) as it does not cost elastic energy to perform a rotation at  $q=0$ . In practice, this divergence is avoided by a large scale cut off given by the sample size or by a finite (electric or magnetic) field.

Samples of macroscopically oriented nematic liquid crystals look turbid, although much less so than nonoriented samples. The multiple scattering from unoriented samples has not been studied in detail so far and we thus focus on dynamic multiple light scattering from the former [56\*,57,58]. In the above model, the low- $q$  divergence of the static structure factor results in a vanishing scattering mean free path  $\tau_s$ , whereas the transport mean free path  $\tau^*$  stays finite. The photon diffusion constant becomes anisotropic and the orientationally averaged value of  $\tau^*$  is of the order  $(\delta\epsilon/\epsilon)^2 \kappa/(kTk_0^2)$  [56\*,57,58]. On scales much larger than  $\tau^*$ , we therefore recover the (anisotropic) photon diffusion picture, and, for not too large anisotropy  $\delta\epsilon/\epsilon$  the dynamic correlation function  $g_1(t)$  can be written in a form very similar to Equation 1. Note, however, that the contributions of paths of length  $s$  cannot be considered as independent contributions of  $s/\tau_s$  scattering events at average distance  $\tau_s$ , as  $\tau_s$  and the associated relaxation rate vanish together. On the 'natural' length scale  $\tau^*$ , we find the 'natural' relaxation rate  $\kappa k_0^2/\eta$ . Some of the features of  $g_1(t)$  predicted by this model [56\*,58] have been tested in a first DWS experiment [57].

#### Imaging objects with distinct dynamics in multiple scattering media

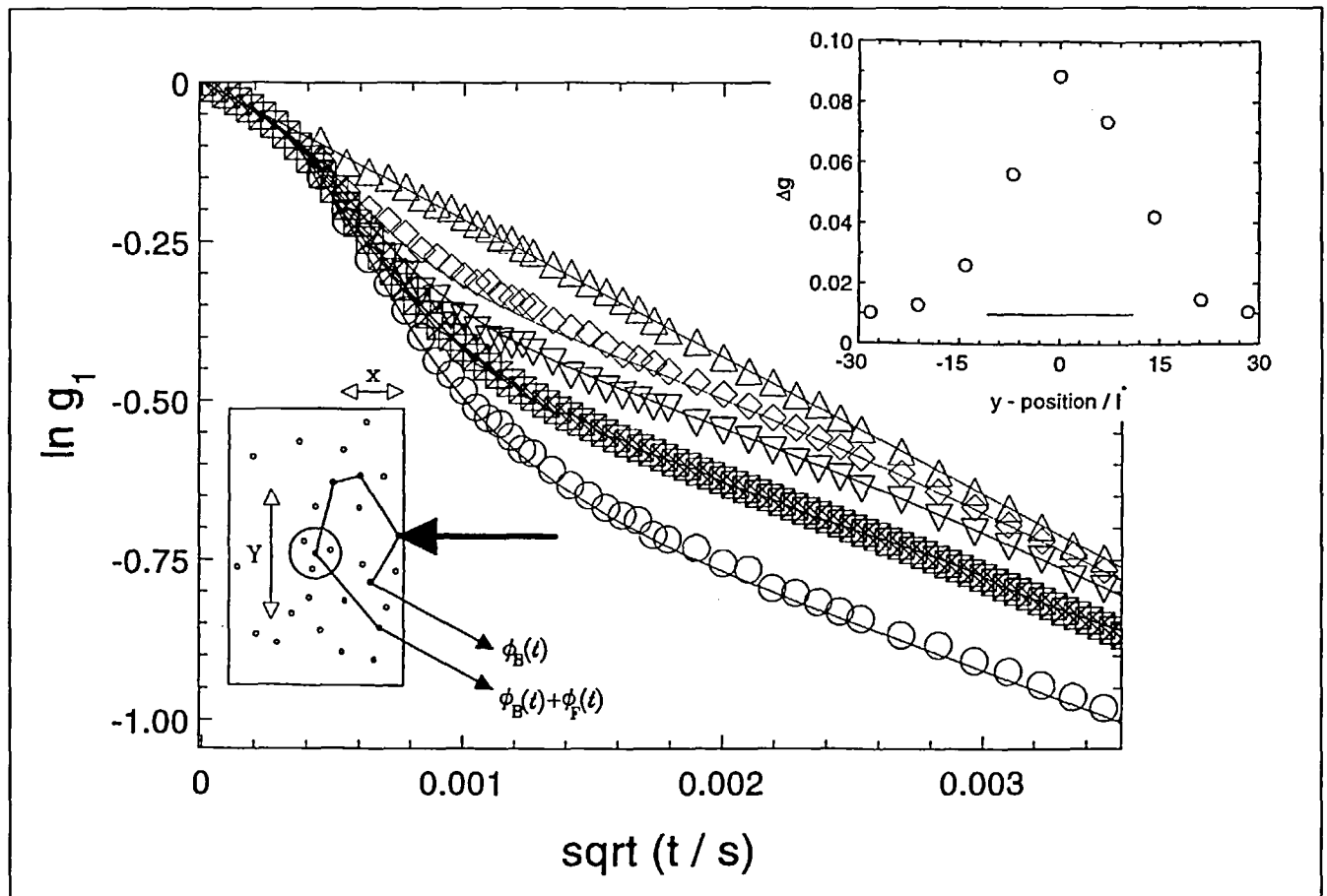
In recent years, there has been substantial progress made in optical imaging 'beyond the transport mean free path' (see [59,60] and references therein). Various techniques, such as interferometric detection of the weak, unscattered coherent beam, time-resolved selection of early arriving (almost) unscattered photons, or measurements of photon density waves and diffuse photon intensities, have been applied [60] in order to locate and eventually image objects which are buried several optical transport mean free paths deep inside the medium. In this work [60], the optical contrast of the object, with respect to the turbid medium, is due to enhanced transparency or enhanced absorption both of which modify the spatial distribution of the diffuse light intensity. The object basically acts as a source or a sink for diffusing photons and therefore generates a glow or a shadow, respectively, on the sample surface. Glow or shadow are less in amplitude, but larger in size for

deeply buried objects than for objects near the surface, because of the diffusive spread of photons from the object to the surface. This allows the localization of the object. The spatial resolution degrades roughly linearly with the distance of the object from the surface [61].

This principle can also be used to image or locate objects which have dynamic contrast because of some motion with respect to the surrounding medium. Although in this case the average scattered intensity does not necessarily depend on the position at the sample surface, the temporal fluctuations of it, as seen in  $g_1(t)$ , do. This idea was suggested by work on speckle tomography [62] which pointed out the fact that if scatterers are moved even a small distance, the corresponding changes of the speckle pattern are most pronounced in the surface region closest

to them. Boas *et al.* [63,64\*] reported images of a spherical cavity containing a colloidal suspension in Brownian motion (with  $\tau^* = 1.5$  mm), located 0.75 diameters below the surface of a solid multiple scattering medium (with  $\tau^* = 2.2$  mm). In this case, there was contrast both in scattering and in dynamics. Heckmeier *et al.* [65,66\*,67] have performed experiments on objects having different types of purely dynamic contrast (i.e. identical  $\tau^*$  values inside and outside the object). Position-dependent  $g_1(t)$  measurements [65], made on a capillary containing a flowing colloidal suspension embedded in the same suspension undergoing Brownian motion, revealed that flow rate, depth and in plane location of the object can be obtained, and  $g_1(t)$  is in excellent agreement with simple photon-diffusion theory [66\*]. An example is shown in Figure 2. The dynamic contrast has a maximum for a

Figure 2



Example of dynamic multiple scattering imaging: an object containing scatterers, which undergo differential motion with respect to the surrounding multiple scattering medium, can be localized and imaged using DWS. A capillary (of 1.5 mm diameter) containing a concentrated colloidal suspension (0.12  $\mu\text{m}$  diameter polystyrene latex particles in aqueous suspension at 5.8% volume fraction,  $\tau^* = 67 \mu\text{m}$ ) is buried inside a  $5/4/2 \text{ cm}^3$  cell filled with the same suspension. The suspension inside the capillary flows at a rate of  $0.5 \text{ ml s}^{-1}$ . Some of the diffusing light picks up dynamic phase shifts  $\phi_F(t)$  due to flow, in addition to the phase shifts  $\phi_B(t)$  caused by Brownian motion. The corresponding decay of  $g_1(t)$  is more pronounced when the capillary is located at a smaller distance ( $x$ ) from the surface of the cell ( $x=2.8\tau^*$  (O),  $x=4.2\tau^*$  ( $\square$ ),  $x=5.7\tau^*$  ( $\nabla$ ),  $x=7.1\tau^*$  ( $\diamond$ ),  $\Delta$ =no flow). The maximum flow-induced change  $\Delta g$  of  $g_1(t)$  clearly shows the lateral ( $y$ ) position of the capillary, which is also indicated as a horizontal line in the inset. Adapted with permission from [66\*].

well defined correlation time  $\tau$ . This is because  $g_1(t)$  at very short times is dominated by Brownian motion (which is, of course, identical inside and outside the object) as compared to flow, whereas at very long times only scattering paths too short to sense the embedded object contribute to  $g_1(t)$ . It is also possible to obtain dynamic contrast between Brownian particles having different sizes [66\*]. In the particularly sensitive situation that the  $g_1(t)$  measurement is made on a dark spot of the static speckle of a solid background medium containing a dynamic inclusion undergoing Brownian motion or flow, objects could be located as deep as five diameters and more than  $30\tau^*$  inside [67]. Finally, the probability distribution of the scattered intensity sampled at long times rather than the full time dependence of  $g_1(t)$  can be used for imaging purposes.

The above principles are expected to turn out to be useful for many applications, in particular, in biomedical sciences. This may be illustrated by a recent experiment [64\*] on superficial burns of animal tissues, where indications about the depth of burn could be obtained from the analysis of the temporal decay of  $g_1(t)$ ; the superficially burned layer of tissue behaves like a solid, whereas the nonburned tissue below generates time-dependent speckle fluctuations due to blood flow.

## Conclusions

DWS has become a very useful tool to probe dynamical properties of multiple scattering media of various kinds. Studies on calibrated colloidal suspensions have born out the potential of DWS to investigate fundamental problems in the physics of fluids, as illustrated, for instance, by the observation of the short-time motion of spherical particles governed by hydrodynamic interactions [20–22]. Many novel contributions of DWS to divers problems in statistical physics are expected, primarily because of the wide range of time and distance scales covered. The quantitative understanding of DWS will now allow one to tackle more complex systems. Foams, sand, liquid crystals, emulsions, and polymer gels doped with scattering particles have been mentioned briefly and many more applications are foreseen, particularly important perhaps for the quality control of food, cosmetics and paints. Multiple scattering imaging and remote sensing of buried objects in motion may evolve into a versatile tool of special interest for medical applications, given the relatively low optical extinction of biological tissue in the near infrared and the possibility to select particular objects spectroscopically. Examples include blood vessels, coagulates or dye-stained tumors. Such applications will be complementary to and, with the availability of low cost sources and detectors of light, substantially cheaper than current NMR or X-ray imaging techniques.

## References and recommended reading

Papers of particular interest, published within the annual period of review, have been highlighted as:

- of special interest
  - of outstanding interest
1. Schuster A: *Astrophys J* 1905, 21:1.
  2. Anderson PW: On the question of classical localization: a theory of white paint. *Phil Mag* 1985, 52:505–509.
  3. Van Albada MP, Lagendijk A: Observation of weak localization of light in a random medium. *Phys Rev Lett* 1985, 55:2692–2695.
  4. Wolf PE, Maret G: Weak localization and coherent backscattering of photons in disordered media. *Phys Rev Lett* 1985, 55:2696–2699.
  5. Ivanov DY, Kostko AF: Spectrum of multiply quasi-elastically scattered light. *Opt Spectrosc (USSR)* 1983, 55:950–953.
  6. Golubentsev AA: Suppression of interference effects in multiple scattering of light. *Sov Phys JETP* 1984, 59:26–34.
  7. Maret G, Wolf PE: Multiple light scattering from disordered media: the effect of Brownian motion of scatterers. *Z Phys* 1987, 65:409–413.
  8. Pine DJ, Weitz DA, Chaikin PM, Herbolzheimer E: Diffusing wave spectroscopy. *Phys Rev Lett* 1988, 60:1134–1137.
  9. Pine DJ, Weitz DA, Maret G, Wolf PE, Herbolzheimer H, Chaikin PW: Dynamical correlations of multiply scattered light. In *Scattering and Localization of Classical Waves in Random Media*. Edited by Sheng P. Singapore: World Scientific; 1990:312–372.
  10. Weitz DA, Pine DJ: Diffusing wave spectroscopy. In *Dynamic Light Scattering*. Edited by Brown W. New York: Oxford University Press; 1993:652–720.
  11. Schätzel K, Drewel M, Ahrens J: Suppression of multiple light scattering in photon correlation spectroscopy. *J Phys Condens Matt* 1990, 2:393–398.
  12. Wiese H, Horn D: Single mode fibers in fiber-optic quasielastic light scattering: a study of the dynamics of concentrated latex dispersions. *J Chem Phys* 1991 94:6429–6443.
  13. Dhadwal HS, Ansari RR, Meyer WV: A fiber-optic probe for particle sizing in concentrated suspensions. *Rev Sci Instrum* 1991, 62:2963–2968.
  14. Van Keuren ER, Wiese H, Horn D: Diffusing-wave spectroscopy in concentrated latex dispersions: an investigation using single-mode fibers. *Colloid Surf A* 1993, 77:29–37.
  15. Durian DJ: The accuracy of diffusing-wave spectroscopy theories. *Phys Rev E* 1995, 51:3350–3358.
  16. Zhu JX, Pine DJ, Weitz DA: Internal reflection of diffusive light in random media. *Phys Rev A* 1991, 44:3948–3959.
  17. Nieuwenhuizen ThM, Luck JM: The skin layer of diffusive media. *Phys Rev E* 1993, 48:569–579.
  18. Kaplan PD, Kao MH, Yodh AG, Pine DJ: Geometric constraints for the design of diffusing-wave spectroscopy experiments. *Appl Optic* 1993, 32:3828–3836.
  19. Durian D: Influence of boundary reflections and refraction on diffusive photon transport. *Phys Rev E* 1994, 50:857–866.
  20. Weitz DA, Pine DJ, Pusey PN, Tough RJA: Nondiffusive Brownian motion studied by diffusing-wave spectroscopy. *Phys Rev Lett* 1989, 63:1747–1750.
  21. Zhu JX, Durian DJ, Müller J, Weitz DA, Pine DJ: Scaling of transient hydrodynamic interactions in concentrated suspensions. *Phys Rev Lett* 1992, 68:2559–2562.
  22. Kao MH, Yodh AG, Pine DJ: Observation of Brownian motion on the time scale of hydrodynamic interactions. *Phys Rev Lett* 1993, 70:242–245.
  23. Ladd AJC, Gang H, Zhu JX, Weitz DA: Time dependent collective diffusion of colloidal particles. *Phys Rev Lett* 1995, 74:318–321.

24. Ladd AJC, Gang H, Zhu JX, Weitz DA: Temporal and spatial dependence of hydrodynamic correlations: simulation and experiment. *Phys Rev E* 1995, 52:6550–6572.
25. Espagnol P, Rubio MA, Zuniga I: Scaling of the time-dependent self-diffusion coefficient and the propagation of hydrodynamic interactions. *Phys Rev E* 1995, 51:803–806.
- This paper resolves the apparent paradox raised by [21], that colloidal particles moving in suspension 'feel' neighbors already at timescales too short for the hydrodynamic interaction to propagate the average interparticle distance. In fact, an important part of the velocity correlation propagates with the speed of sound, which is much faster than the diffusion of vorticity.
26. MacKintosh FC, John S: Diffusing wave spectroscopy and multiple scattering of light in correlated random media. *Phys Rev B* 1989, 40:2383–2406.
27. Fraden S, Maret G: Multiple light scattering from concentrated interacting suspensions. *Phys Rev Lett* 1990, 65:512–515.
28. Qiu X, Wu XL, Xue JZ, Pine DJ, Weitz DA, Chaikin PM: Hydrodynamic interactions in concentrated suspensions. *Phys Rev Lett* 1990, 65:516–519.
29. Xue JZ, Wu XL, Pine DJ, Chaikin PM: Hydrodynamic interactions in hard-sphere suspensions. *Phys Rev A* 1992, 45:989–993.
30. Kaplan PD, Yodh AG, Pine DJ: Diffusion and structure in dense binary suspensions. *Phys Rev Lett* 1992, 68:393–396.
31. Nilson SJ, Gast AP: The influence of structure on diffusion in screened coulombic suspensions. *J Chem Phys* 1994, 101:4975–4985.
32. Meller A, Stavans J: Glass transition and phase diagrams of strongly interacting binary colloidal mixtures. *Phys Rev Lett* 1992, 68:3646–3649.
33. Sanyal S, Sood AK, Ramkumar S, Ramaswamy S, Kumar N: Novel polarization dependence in diffusing-wave spectroscopy of crystallizing colloidal suspensions. *Phys Rev Lett* 1994, 72:2963–2966.
34. Dinsmore AD, Yodh AG, Pine DJ: Phase diagrams of nearly hard-sphere binary colloids. *Phys Rev E* 1995, 52:4045–4057.
35. Wu XL, Pine DJ, Chaikin PM, Huang JS, Weitz DA: Diffusing-wave spectroscopy in a shear flow. *J Opt Soc Am B* 1990, 7:15–20.
36. Bicout D, Akkermans E, Maynard R: Dynamical correlations for multiple scattering in laminar flow. *J Phys I* 1991, 1:471–491.
37. Bicout D, Maret G: Multiple light scattering in Taylor-Couette flow. *Physica A* 1994, 210:87–112.
38. Bicout D, Maynard R: Multiple light scattering in turbulent flow. *Physica B* 1995, 204:20–28.
39. Ginder JM: Diffuse optical probes of particle motion and structure formation in an electrorheological fluid. *Phys Rev E* 1993, 47:3418–3429.
40. Leutz W, Maret G: Ultrasonic modulation of multiply scattered light. *Physica B* 1995, 204:14–19.
41. Gang H, Krall AH, Weitz DA: Shape fluctuations of interacting fluid droplets. *Phys Rev Lett* 1994, 73:3435–3438.
42. Gang H, Krall AH, Weitz DA: Thermal fluctuations of the shapes of droplets in dense and compressed emulsions. *Phys Rev E* 1995, 52:6289–6302.
43. Mason TG, Weitz DA: Optical measurements of frequency-dependent linear viscoelastic moduli of complex fluids. *Phys Rev Lett* 1995, 74:1250–1253.
- Although the physics of their observations remains to be worked out in more detail, the authors report on the striking possibility of measuring the viscoelastic moduli of various complex turbid fluids with DWS over a wide frequency range. See also [44].
44. Mason TG, Weitz DA: Diffusing-wave-spectroscopy measurements of viscoelasticity of complex fluids. *J Opt Soc Am A* 1997, 14:139–149.
45. Mason TG, Gang H, Weitz DA: Rheology of complex fluids measured by dynamic light scattering. *J Molec Struct* 1997, in press.
46. Durian DJ, Weitz DA, Pine DJ: Multiple light-scattering probes of foam structure and dynamics. *Science* 1991, 252:686–688.
47. Durian DJ, Weitz DA, Pine DJ: Scaling behavior in shaving cream. *Phys Rev A* 1991, 44:7902–7905.
48. Earnshaw JC, Jaafar AH: Diffusing wave spectroscopy of a flowing foam. *Phys Rev E* 1994, 49:5408–5411.
49. Gopal AD, Durian DJ: Nonlinear bubble dynamics in a slowly driven foam. *Phys Rev Lett* 1995, 75:2610–2613.
50. Earnshaw JC, Wilson M: A diffusing wave spectroscopy study of constrictive flow of foam. *J Phys II* 1996, 6:713–722.
51. Gopal AD, Durian DJ: Fast thermal dynamics in aqueous foams. *J Opt Soc Am A* 1997, 14:150–155.
52. Horne DS, Davidson CH: The use of dynamic light scattering in monitoring rennet formation. *Milchwissenschaft* 1990, 45:712.
53. Kaplan PD, Yodh AG, Townsend DF: Noninvasive study of gel formation in polymer-stabilized dense colloids using multiply scattered light. *J Colloid Interface Sci* 1993, 155:319–324.
54. Xue JZ, Herbolzheimer E, Rutgers MA, Russel WB, Chaikin PM: Diffusion, dispersion and settling of hard spheres. *Phys Rev Lett* 1992, 69:1715–1718.
55. Menon M, Durian DJ: The dynamics of grains in flowing sand. •• *Science* 1997, 275:1920–1922.
- A very interesting DWS study on a novel type of dynamic multiple scattering system: flowing sand. Various dynamic processes on the microscopic scale are discovered and quantitatively described.
56. Stark H, Lubensky TC: Multiple light scattering in nematic liquid crystals. • *Phys Rev Lett* 1996, 77:2229–2232.
- The first theoretical description of the dynamic multiple light scattering from an oriented nematic liquid crystal. See also [57] and [58].
57. Kao MH, Jester KA, Yodh AG, Collings PJ: Observation of light diffusion and correlation transport in nematic liquid crystals. *Phys Rev Lett* 1996, 77:2233–2236.
58. Stark H, Kao MH, Jester KA, Lubensky TC, Yodh AG: Light diffusion and diffusing-wave spectroscopy in nematic liquid crystals. *J Opt Soc Am A* 1997, 14:156–178.
59. Yodh AG, Chance B: Spectroscopy and imaging with diffusing light. *Phys Today* 1995, 48:34–40.
60. Alfano RR (Ed): *OSA Proceedings on Advances in Optical Imaging and Photon Migration*, vol 21. Washington DC: Optical Society of America: 1994.
61. DenOuter PN, Nieuwenhuizen ThM, Lagendijk A: Location of objects in multiple scattering media. *J Opt Soc Am A* 1993, 10:1209–1218.
62. Berkovits R, Feng S: Theory of speckle tomography in multiple-scattering media. *Phys Rev Lett* 1990, 65:3120–3123.
63. Boas DA, Campbell LE, Yodh AG: Scattering and imaging with diffusing temporal field correlation. *Phys Rev Lett* 1995, 75:1855–1858.
64. Boas DA, Yodh AG: Spatially varying dynamical properties of turbid media probed with temporal light correlation. • *J Opt Soc Am A* 1997, 14:192–205.
- A nice illustration of how the recently developed concept of flow visualization and imaging [63,65,66\*,67] can be applied to some biomedical problems, here, to the determination of depth of burns.
65. Heckmeier M, Maret G: Visualization of flow in multiple-scattering liquids. *Europhys Lett* 1996, 34:257–262.
66. Heckmeier M, Skipetrov SE, Maret G, Maynard R: Imaging of dynamic heterogeneities in multiple-scattering media. • *J Opt Soc Am A* 1997, 14:185–191.
- This paper shows that motions of scatterers, confined to an inclusion embedded into scatterers undergoing other motions, can be visualized even under conditions of strong multiple scattering, and gives these measurements a quantitative grounding by comparison with a diffusion theory. See also [62,64\*].
67. Heckmeier M, Maret G: Dark speckle imaging of colloidal suspensions in multiple light scattering media. *J Colloid Interface Sci* 1997, in press.